Organic matter accumulation and preservation controls in a deep sea modern environment: an example from Namibian slope sediments.

Laetitia Pichevin, Philippe Bertrand, Mohammed Boussafir, Jean-Robert Disnar

Organic matter accumulation and preservation controls in a deep sea modern environment: an example from Namibian slope sediments

Laetitia Pichevin [a], Philippe Bertrand [a], Mohammed Boussafir [b] and

Jean-Robert Disnar [b]

[a] Département de Géologie et Océanographie, Université Bordeaux I, UMR-CNRS 5805, 33405, Talence Cedex, France
[b] Laboratoire de Géologie de la Matière Organique, Institut des Sciences de la Terre d'Orléans (I.S.T.O.), UMR-CNRS 6113, BP 6759, 45067, Orléans Cedex 2, France

Abstract

The Lüderitz upwelling cell is presently the most productive area of the Benguela current system and abundant organic matter (OM) accumulates on the adjacent slope sediments even at great water depth. OM from two cores taken on the slope and covering the last 280 kyear was analysed in terms of "petroleum quality" (Rock-Eval), chemical features (FTIR, EDS) and petrographic composition (light microscopy and TEM). These data indicate that the OM is more oxidized at 3606 m water depth than on the upper slope sediments (1029 m) although the petroleum quality of the OM throughout the deep-water core remains surprisingly high for hemipelagic deep-sea sediments (HI=200–400 mg/g). The petroleum quality of OM accumulated on the upper slope is consistently high: HI averages 450 mg/g. Two petrographic types of OM are distinguishable from microscopic observation, each ascribed to distinctive preservation mechanisms: (1) 'Granular' amorphous OM, which dominates in the deep-water core, is formed by organo-mineral aggregates. Aggregation appears to be the primary preservation mode at this depth although is quantitatively limited (maximum TOC value of 4 wt.% of bulk sediment obtained through this process). The ultrastructure of the aggregates highlights an intimate association pattern between sedimentary OM and clays. (2) 'Gel-like' nannoscopically amorphous OM (NAOM) largely dominates at 1000 m water depth and contains sulfur. Thus, early diagenetic sulfurization was probably involved in the preservation of this OM, but a contribution from the classical degradation–recondensation pathway cannot be ruled out. Moreover, selective preservation occurred at both sites but represents an insignificant part of the OM.

Organic fluxes mainly control the occurrence and extent of sulfurisation at both water depths by determining the redox conditions at the sea floor. Aggregate formation is limited by both organic and mineral fluxes at the lower slope whereas OM supply is never limiting on the upper slope. Although consistently operating through time at both depths, preservation by organo-mineral association is limited by mineral availability and thus accounts for a relatively minor portion of the OM accumulated on this organic-rich slope. In the case of large organic fluxes, sulfurisation and/or

degradation–recondensation is required to obtain TOC contents above 4 wt.% of bulk sediment in the area.

1. Introduction

The degradation of organic matter (OM) spans the journey of dead organisms and detritus as they sink from the euphotic zone through the water column, enter the sediment and are ultimately buried. Degradation processes involve a series of redox reactions that provide electron acceptors for the oxidation of OM by heterotrophs. Oxygen, when present, is energetically favoured over other oxidants and is the first to be consumed. Next, nitrate, Mn/Fe oxides and sulfate are successively consumed in the degradation of any remaining organic compounds (Canfield, 1993).

As in most open ocean regions, the water column overlying the Namibian slope is usually well oxygenated at all depths. However, during highly productive upwelling events, the large amount of exported labile organic matter can cause the rate of O_2 consumption in surface sediments to exceed the supply of dissolved oxygen by diffusion from the bottom water (Calvert and Pedersen, 1993), generating anoxic conditions at the sediment–water interface. Thus, the OM which sediments on the Namibian slope is likely to experience varying degrees of biochemical transformation under oxic, sub-oxic and/or anoxic conditions (Schulz et al., 1994), depending on the flux of labile organic matter that reaches the sea floor.

The aim of this work was to investigate organic matter preservation mechanisms that may have contributed to the high TOC contents measured in slope sediments off Lüderitz, spanning the last 280 kyear. The maximum TOC content in a core from the upper slope (about 1000 m water depth) is ~17% (8% on average) and the maximum value on the lower slope (ca. 3600 m) is as high as 8% (2% on average). The broad range of OC concentrations recorded (from ca. 0.3 to 17.4%) allows the study of various OM preservation states. Moreover, the bathymetric range (1000 vs. 3600 m water depth) and long time scale permit a test of the impact of (1) water depth, in terms of sinking time and distance from the coast, and (2) climate, through sea level and primary productivity changes. Through assessment of petroleum quality, petrographic composition and some chemical features of the OM, we have determined the preservation processes that occurred on the Lüderitz slope and their variation with depth and time.

2. Rationale

Organic compounds exported from the euphotic zone can be classified into two main types by considering their ‘preservation potential’ (Tegelaar et al., 1989). The first consists of labile biomacromolecules, namely polypeptides and polysaccharides which are prone to intense degradation during transit (e.g. Wakeham et al., 1997). The second, which is resistant or refractory, includes, for example, lignin, tannin and algeanan. The last is found in the cell walls of various algae, e.g. *Botryococcus braunii* and is well preserved in sediments (Derenne et al., 1991 and Derenne et al., 1997). Although resistant biomacromolecules do not dominate biomass, they become

increasingly concentrated with increasing time in the water column or decreasing burial efficiency, while the more labile molecules are degraded (Largeau et al., 1984; Largeau et al., 1986; Largeau et al., 1989 and Hedges et al., 2001).

Labile organic matter can become more resistant owing to chemical transformation during sinking and early diagenesis. The 'degradation-recondensation' pathway (Tissot and Welte, 1984) consists of successive and random repolymerization and polycondensation reactions acting on the degradation products (monomers) of the original OM. Another mechanism, the so-called natural sulfurization process, has been well described by Sinninghe-Damsté et al., 1989; Lückge et al., 1996 and Lückge et al., 2002, among others, for both ancient sediments and recent environments. This preservation pathway involves the protective role of newly formed bonds between S and functionalized OM. Under anoxic conditions, inorganic sulfur species produced by sulfate reduction are scavenged by iron to form pyrite. When the amount of sulfides formed exceeds that which can be fixed as pyrite, the surplus may re-oxidize or be incorporated into OM (Lückge et al., 2002). These reactions take place during the early diagenetic stages (Schouten et al., 1994; Wakeham et al., 1995 and Adam et al., 2000) and form characteristic molecules such as isoprenoid thiophenes (Sinninghe-Damsté et al., 1989 and Kok et al., 2000).

Over the past 20 years, a fourth preservation pathway, the so-called protection by mineral matrix, has been evidenced in soils (Oades, 1988), sedimentary rocks (Salmon et al., 2000) and recent marine sediments (e.g. Mayer et al., 1985; Keil et al., 1994a; Mayer, 1993; Mayer, 1994; Mayer, 1999; Ransom et al., 1997; Hedges and Keil, 1999 and Armstrong et al., 2002). Suess (1973) noted that the highest organic carbon contents in some recent marine environments correlate with a low mean grain-size of the mineral fraction. Mayer et al. (1988) proposed that high specific surface area, rather than the fine-grained texture of the sediment, inhibits degradation by increasing the amount of OM that could be protected by adsorption on to mineral particles. Mesopore spaces (<10 nm in diameter) and the interstices of siliciclastic particles, which represent 80% of the sediment surface area, constitute the most efficient traps for OM and prevent its degradation by excluding enzymatic hydrolysis (Mayer, 1994 and Bock and Mayer, 2000). Among the classic siliciclastic minerals in marine sediments and soils, OM is preferentially associated with clays, (Mayer, 1994 and Keil et al., 1994b), especially the Ca-rich clays of the smectite group (Furukawa, 2000). The latter study also showed that OM is associated with the surfaces as well as being structurally incorporated into clay crystals. OM is not systematically coated on grain surfaces and pores as thin layers or infillings, but can appear as blebs Ransom et al., 1997; Ransom et al., 1998a and Ransom et al., 1998b. Organo-mineral associations can also occur as alternating organic and clay nanolayers, as evidenced in Cenomanian black shales (Salmon et al., 2000).

3. Study area and sediment composition

The Benguela upwelling system is one of the four major eastern boundary current regions in the world and is characterized by cold, nutrient-rich sub-surface water which upwells owing to prevailing southeasterly trade winds. The upwelling area is composed of several distinct upwelling cells (Lutjeharms and Meeuwis, 1987), distributed from the Angola-Benguela front to the Agulhas retroflection zone, which constitute its northern and southern boundaries, respectively (Fig. 1). Perennially

consistent atmospheric conditions maintain the activity of the central Walvis and Lüderitz cells (22–27° S, Shannon and Nelson, 1996) while southern cells show a stronger seasonality. Productivity measured along the Lüderitz and Walvis coasts is one of the highest in the world and often reaches 350 gCm^{-2} $year^{-1}$ (Behrenfeld and Falkowski, 1997).

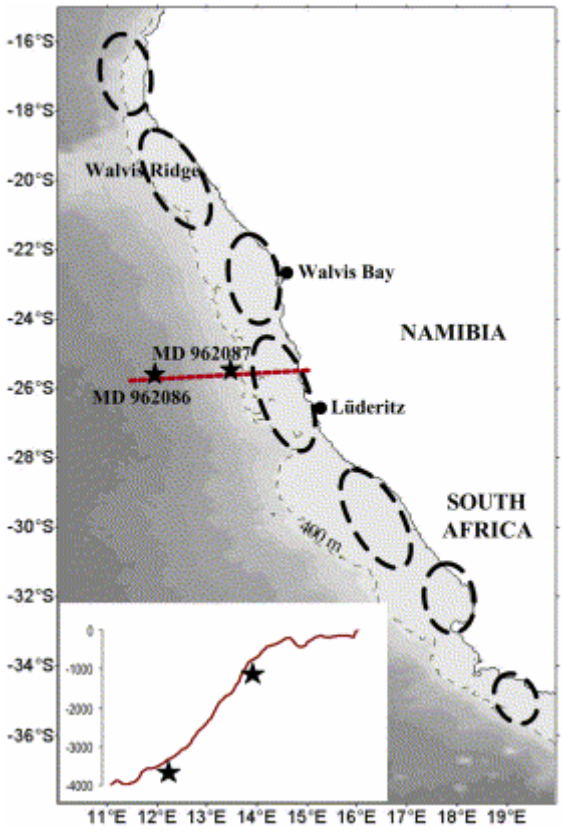

Fig. 1. Core locations, topography of Lüderitz slope and water depths. The dashed isobath underlines the mean depth of the shelf break. The upwelling cells are represented as dashed circles.

A thermal front coincides with the shelf break and constitutes the offshore limit of the upwelling cell, though a filamentous mixing domain streaming up to 1000 km offshore in winter allows highly productive conditions well beyond the front (Lutjeharms and Meeuwis, 1987 and Hagen et al., 2001). The most productive zones do not systematically occur within the main upwelling centre but on the outer fringe of the cell (Mollenhauer et al., 2002). It has been documented that, under strong wind-stress conditions, a secondary upwelling cell may occur seaward of the front (Barange and Pillar, 1992 and Giraudeau and Bailey, 1995).

The prevailing wind field parallels the coastline. Thus, aeolian transport of detrital material from the arid continent to the ocean is weak and terrigenous input represents a minor fraction of the sediment. Terrigenous organic matter is, therefore, negligible in the cores studied as shown by the δ^{13}Corg record ranging from −19.5 to −21.4‰ (Martinez, unpublished data).

4. Analytical methods

4.1. Samples

Sediment sampling was carried out in 1996 on the R/V Marion Dufresne during the NAUSICAA cruise using piston-cores of 40 m length. The first core MD962086 (site 25.8° S, 12.13° E) was located at 3606 m water depth and the MD962087 (25.6° S, 13.38° E) lies under 1029 m water depth, on the upper slope (Fig. 1). Both cores were studied over intervals spanning the last 280 kyear, covering two complete climatic cycles. Sampling resolution for TOC measurements (elemental analysis) and Rock-Eval pyrolysis was 10 cm. Petrographic observations and infrared analyses were performed on a selection of samples chosen by TOC content, petroleum quality and location within a climatic cycle; optimum or transition (Fig. 2 and Table 1).

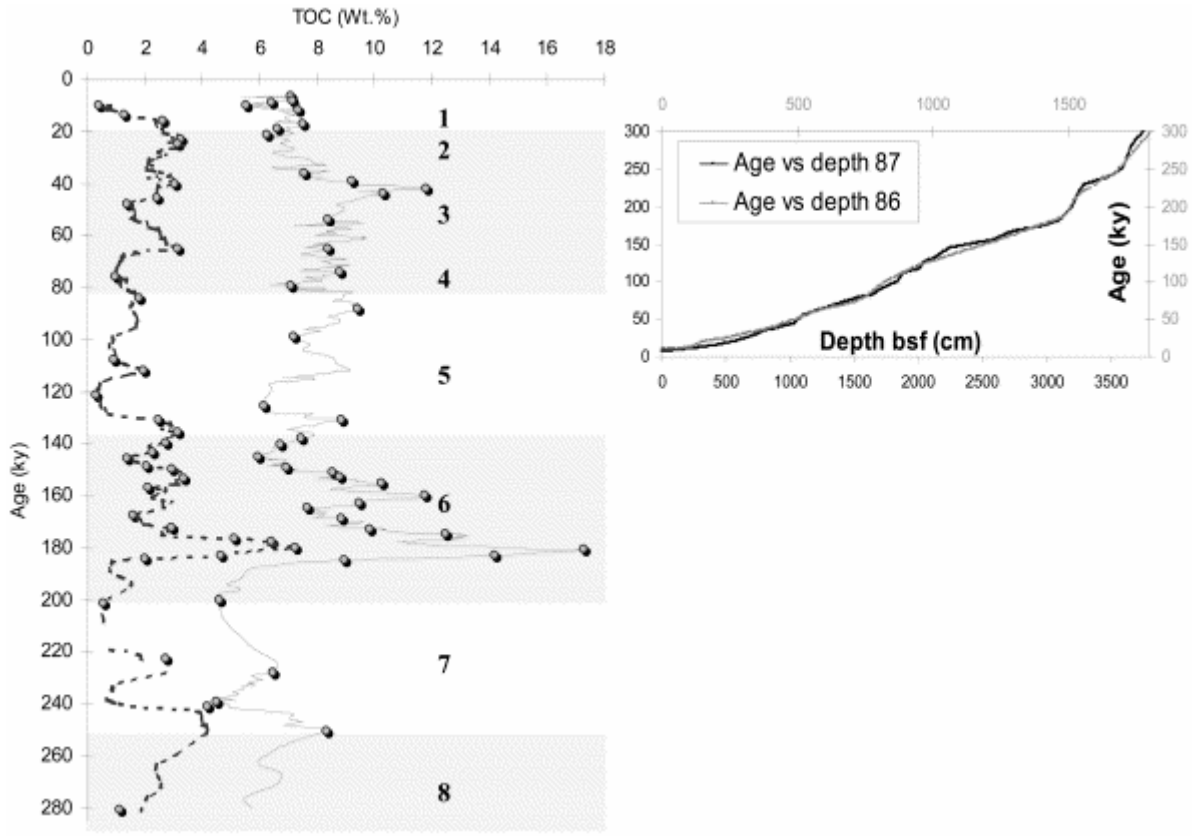

Fig. 2. TOC content vs. age for MD 962086 (dashed line) and MD 962087 (black line). Grey dots represent samples observed by light microscopy. Glacial isotopic stages 2, 3, 4, 6 and 8 are indicated by grey bands, interglacial isotopic stages 1, 5 and 7 by white bands.

Sample	TOC (wt.%)	HI (mg/g)	NAOM (%)	Aggregate (%)	Iox	Water depth (m)
1343	1.6	229	8	80.6	7.03	3606
1439	7.2	349	37.7	57.6	3.5	3606
1513	0.56	200	6.9	61.9	12.8	3606
120	6.4	424	38.7	55.9	2.02	1029
990	11.8	470	75.2	19.5	1.85	1029
3102	17.3	329	87.7	8.8	1.85	1029

Table 1. Chemical parameters and palynological composition of samples observed by TEM

4.2. Stratigraphy

The age model at site MD962086 was generated by correlation of the benthic foraminifera species *Cibicidoides wuellerstorfi* $\delta^{18}O$ records with the SPECMAP reference (Imbrie et al., 1984), as given by Bertrand et al. (2003) with slight modification. No oxygen isotope data were available for MD962087 because of carbonate dissolution. The age model for MD962087 was obtained by seven radiocarbon measurements on tests of mixed planktonic foraminifers (Arizona AMS facility, USA and Gif, France) for the last 40 kyear (Table 2). A polynomial calibration with the Calib 4.3 program (Stuiver et al., 1998) and a regional reservoir correction of 400 years were applied for all ^{14}C dates. The chronology of earlier stages of MD 962087 was obtained by correlation of TOC and $CaCO_3$ records with those of MD962098, MD962086 (Lüderitz transect) and GEOB 1712-4 (Walvis Bay, 998 m water depth) published by Kirst et al. (1999).

Reference	Depth bsf (cm)	AMS Age (years)	Error (years)	Species	Calendar Age (years)
101 217	2	5820	80	Mixed plankton	6177
101 218	199	10,150	90	Mixed plankton	11,009
AA47 704	366	11,336	75	Mixed plankton	12,738
101 219	450	13,890	120	Mixed plankton	15,843
AA47 703	654	20,220	150	Mixed plankton	23,371
101 220	719	26,100	260	Mixed plankton	30,148
101 221	869	35,010	570	Mixed plankton	40,019

Table 2. Radiocarbon dates (MD962087)

4.3. Chemical and spectroscopic analyses

Rock-Eval pyrolysis was performed on 40–60 mg of bulk sediment. Hydrogen indices (HI) was determined using a Rock-Eval VI under a He atmosphere, following the commonly used programme for recent sediments: 400 °C for 3 min, followed by a temperature increase at a rate of 30 °C/min to 750 °C. In 10 carbonate-rich samples, $CaCO_3$ was removed by mild HCl leaching (10% during 1 min) before pyrolysis.

FTIR spectra were obtained on isolated OM samples using a Perkin-Elmer FTIR 16PC spectrometer (following HF/HCl hydrolysis). Each KBr pellet contained 1 mg of isolated OM.

4.4. Petrographic studies

Mineral constituents were eliminated via classical HF/HCl treatment (Durand and Nicaise, 1980). The petrographic features of 72 samples of isolated OM were determined by light microscopy. We obtained qualitative and quantitative descriptions of OM from the shallow and deep cores, i.e. determination of the different organic fractions considering their textural and structural appearance, the contribution of each fraction and pyrite occurrence. The abundance of OM facies was estimated by counting the fraction of the palynofacies slide covered by each facies.

The next step was performed using transmission electron microscopy (TEM) and elemental diffraction analysis (EDS), which permit observation of the structural patterns and the compositional elements of OM at a very fine scale (to 10 nm). The six samples studied by TEM were fixed in osmium tetroxide and embedded in resin as previously described by Boussafir et al. (1994). They were selected according to light microscopy examination and TOC content. To ensure that the observations were representative, three preparations were made and examined for each sample.

5. Results and interpretation

5.1. Petroleum quality: impact of water depth and OC content

Interestingly, TOC values (wt.%) vary significantly with climate: enhanced TOC generally occurs during glacial periods (Fig. 2) and especially during stage 6.6 at both locations. TOC is always much higher for the upper slope samples. In total, 550 samples of bulk sediment from both cores were analysed by Rock-Eval pyrolysis. The results are shown in Fig. 3. HI (mg/g) represents the mass of hydrocarbon compounds produced by pyrolysis of 1 g of TOC. Here, 99% of the HI values range from 150 to 540 mg/g, which demonstrates the variable petroleum quality of the OM. Schematically, high HI indicates that the contribution of hydrocarbon chains (aliphatic compounds) to the total OM is high.

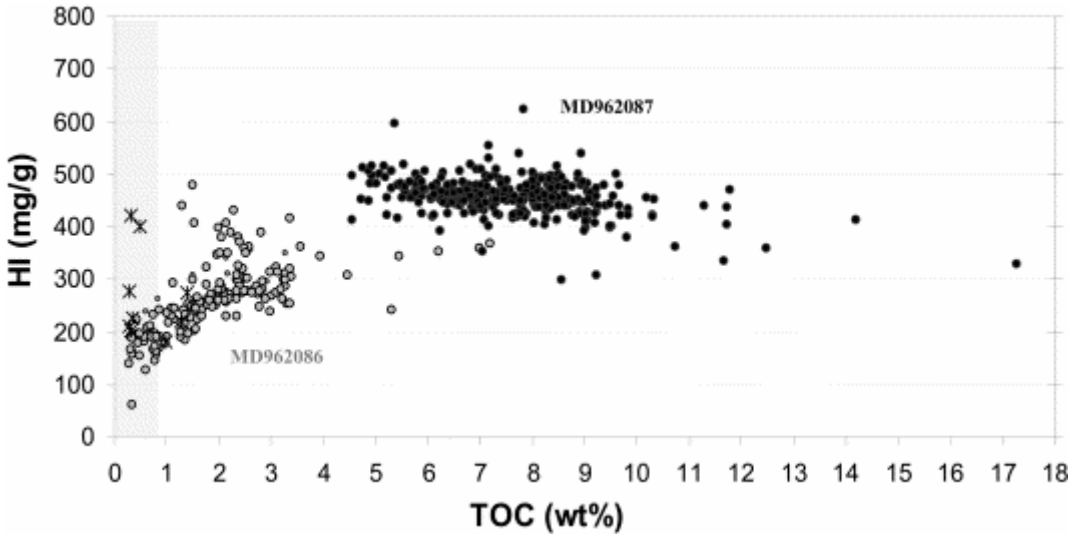

Fig. 3. Hydrogen index (mg/g) vs. TOC (wt.%) for MD 962087 (black) and MD 962086 (grey). High HI indicates more aliphatic compounds. When TOC is under 1%, we assume that HI is underestimated because of carbonate abundance (greater than 70%). Asterisks indicate samples that were examined again after a mild HCl leaching.

As shown in Fig. 3, HI vs. TOC distributions display two different trends depending on the core. The upper slope core MD 962087 shows high, almost constant, HI values (around 450 mg/g) irrespective of the variation in TOC. HI values from the lower slope core (MD 962086) are comparatively lower (50 up to 400) and decrease with decreasing TOC content. The latter core displays the typical decaying trend often described in the literature (e.g. Ramanampisoa and Disnar, 1994). However, when

TOC is under 1%, we assume that HI is underestimated because of the abundance of minerals which can trap the effluents released during pyrolysis (Espitalié et al., 1985 and Saint-Germes et al., 2002). Ten organic-poor samples from the deep core were gently treated with HCl in order to remove carbonate without substantial OM degradation. The HI values of these carbonate-free samples were much higher than those of the untreated ones (200–420 mg/g instead of 50–150 mg/g). Thus, HI values for the deep core range from about 200 to 400 mg/g even when TOC contents are low (<0.5%) and show a weak positive correlation with TOC. On average, for a given TOC value (%), HI is higher in the shallow core than in the deep core.

T_{max} data average 411 °C (±12 and ±25 °C for MD 962087 and 962086, respectively) in agreement with the low maturity of the OM (Espitalié et al., 1985). Oxygen indices (OI mg/g, the mass of CO_2 produced by pyrolysis of 1 g of TOC) range from 120 to 230 mg/g in the shallow core. For the deep core, higher OI values and a wider range are observed: from 130 to more than 700 mg/g. TOC contents are negatively correlated with OI. The highest OI values (from 300 to 700 mg/g), result, however, partly from the thermal decomposition of carbonates, which releases CO_2.

The above results indicate that, at a given location, the petroleum quality of the OM does not vary greatly over 280 kyear despite large variations in TOC. However, HI is substantially higher in the shallow core than in the deep core. OM that reaches the lower slope has presumably remained longer under oxic conditions than the OM accumulated on the upper slope because (1) sinking time increases with water depth and (2) sedimentation rate decreases with increasing distance from the upwelling centre due to decreasing primary productivity (Hedges et al., 1999).

5.2. Petrographic composition

The following palynofacies analyses were performed on a selection of 72 samples in order to depict the petrographic nature of the OM and its variation with climate and water depth. All the samples yield an overwhelming majority of brown/orange, amorphous OM (AOM), and hardly any recognizable palynomorphs. In general, terrestrial plant detritus only accounts for 1–4% of the palynofacies although an enrichment in refractory lignocellulosic debris is observed in samples from the lower slope core with very low TOC content (<1.5 wt.%). We assume that the amorphous OM is of marine origin as suggested by the $\delta^{13}C$ of the OM from MD 962098 averaging −20‰ (Martinez, unpublished data). Framboidal pyrite or single crystals are always present, testifying to the local, permanent occurrence of anoxic conditions in the sediment. Among the amorphous material, two palynological fractions were distinguished (Fig. 4):

1. The granular AOM appears as a pulverulent material formed by clusters of very thin (inframicrometric), irregularly sized curds (Fig. 4b). The texture of the granular AOM is finer in the deep core than in the shallow core sediments.
2. The gel-like AOM consists of discrete or aggregate flecks of a few μm, with clear edges. Each fleck is characterized by a homogeneous texture (Fig. 4c). No trace of biological structure is visible within this amorphous material. This feature recalls the orange AOM described for the Kimmeridgian deposits from Yorkshire (Boussafir et al., 1995 and Boussafir and Lallier-Vergès, 1996) and Orbagnoux (Mongenot et al., 1999). According to these authors, gel-like AOM was produced by sulfurization.

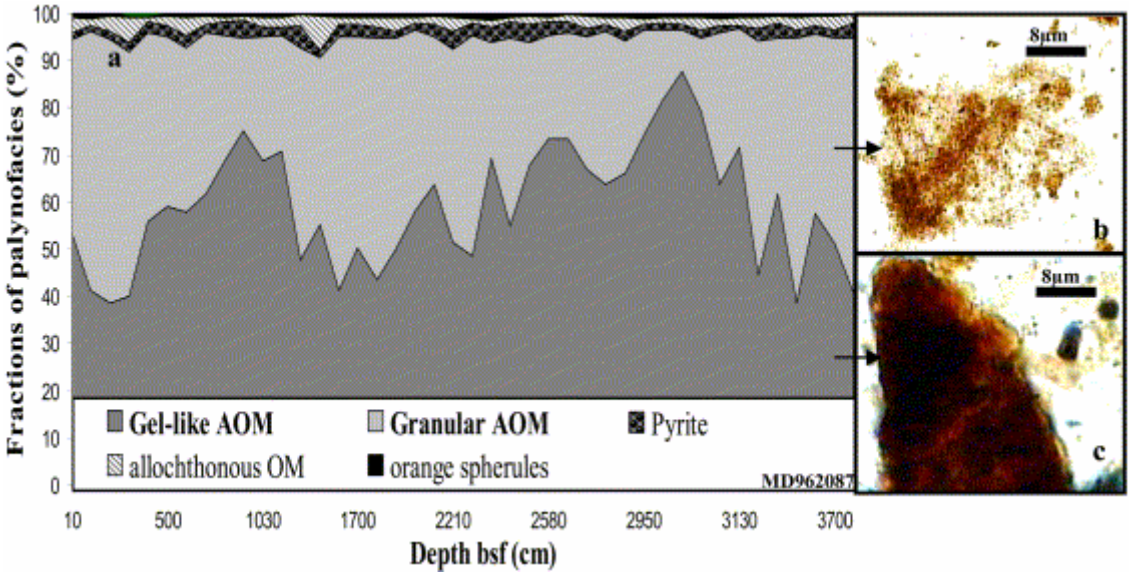

Fig. 4. Light microscopy observations of the isolated OM from MD972087. (a) Palynofacies composition (in% of slide area), (b) Granular Amorphous OM, (c) Gel-like Amorphous OM.

Gel-like AOM is more abundant in the upper slope core (from 40 to 87%) than in the lower slope core (from 3 to 41%) sediments. As a corollary, granular AOM dominates in the palynofacies of MD 962086. Furthermore, gel-like AOM content increases with increasing TOC content and granular AOM abundance follows the opposite trend.

5.3. TEM observations

TEM observations were made on six samples of isolated OM, selected on the basis of the above results. These OM isolates represent samples with TOC contents ranging from 0.56 to 17.4%, including almost completely granular to almost entirely gel-like AOM. Ultra-thin sections of samples 1343, 1439 and 1513 are from the deep core while samples 120, 990 and 3102 come from the shallow core (Table 1). We assume, based on light microscopy observation, that TEM images from samples 3102 and 990 show the nanoscopically amorphous structure of pure gel-like AOM (NAOM), whereas TEM micrographs of samples 1513 and 1343 illustrate the ultrathin structure of granular AOM (Fig. 5). Both types of AOM coexist in samples 120 and 1439, as their TOC contents and petrographic composition are comparable and intermediate. Additionally, EDS analyses were performed on selected OM fractions (Fig. 6a and b). The EDS spectra show the nature of the major elements of the material.

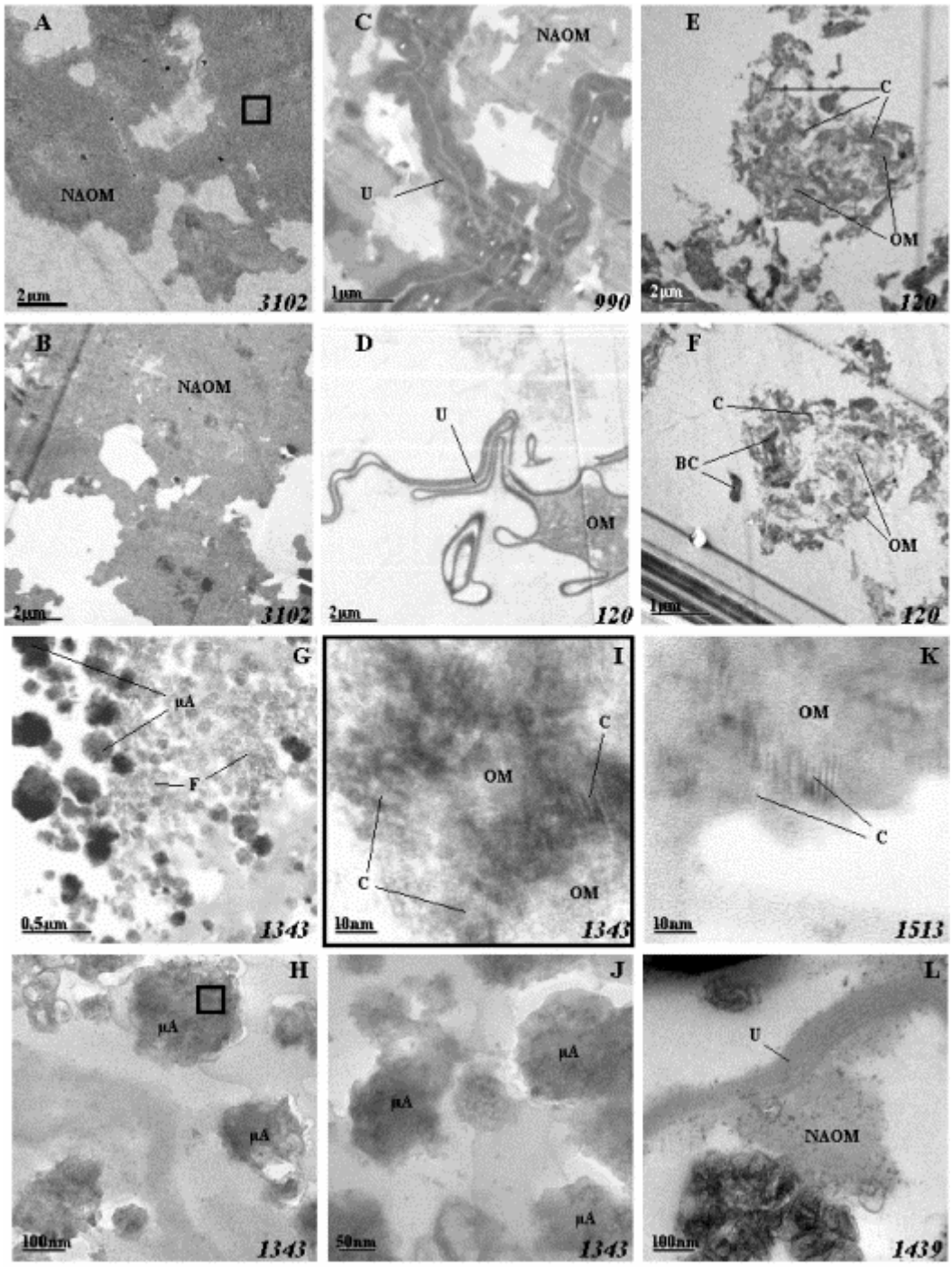

Fig. 5. TEM observations of isolated OM from the shallow core (A–F) and the deep core (G–L). Nanoscopically amorphous organic matter (NAOM) is the major constituent of samples 3102 and 990 (A, B and C). Typical upper slope aggregates involving organic matter (OM), clay (C) and bioclasts (BC) from sample 120 are shown on pictures E and F. Ultralaminae (U) are minor constituents of samples 990 (C) and 120 (D). On the lower slope, NAOM is scarce (L) whereas micro-aggregates (µA) dominate in the three samples: 1343 (G–J), 1439 (L) and 1513 (K). Pictures G, H, J, I and K show the structure of the microaggregates at increasing magnifications. Microaggregates appear homogenous on pictures G, H and J. Higher magnification, however, reveals the ultrastructure of the aggregates: clay lattices are embedded in OM (I and K). (F) indicates 'pale flecks'. The black squares indicate the areas where EDS analyses were performed.

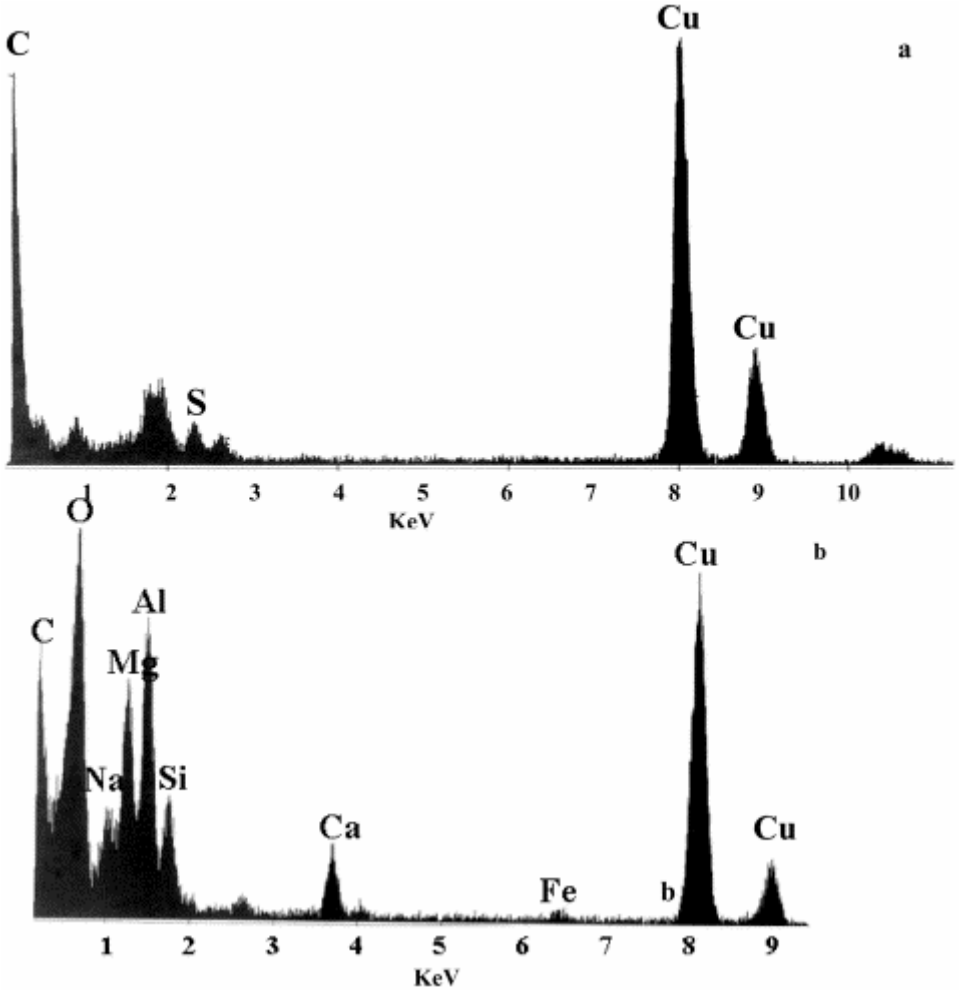

Fig. 6. Typical EDS pin point analyses showing major constituent elements of (a) NAOM and (b) aggregates. The peaks at 8 and 9 keV are due to the copper mount used for the ultrathin-sections.

Gel-like AOM appears as nanoscopically undifferentiated, amorphous smears when viewed by TEM (Fig. 5A, B and C), similar to the orange AOM identified by Boussafir et al., 1995 and Mongenot et al., 1999. Some lamellar structures embedded in NAOM are seen but are not abundant (Fig. 5C and D). These structures are between 7 nm and 50 nm wide and are comparable to the ultralaminae described by Largeau et al. (1989). This indicates that selective preservation exists here but did not play a major role in OM accumulation. Thus, in the ensuing discussion, NAOM will refer to gel-like AOM as this fraction is mainly nanoscopically amorphous. NAOM contains S, as revealed by EDS analysis (Fig. 6a). This suggests preservation by sulfurization, consistent with the conclusions of Boussafir et al., 1995 and Mongenot et al., 1999 concerning the origin of gel-like, orange AOM.

Overall, granular AOM is formed by microaggregates, clusters of microaggregates and pellets. The size and shape of the aggregates vary depending on the core (Fig. 5), i.e. on water depth of deposition, as discussed below. Aggregates are formed by association between OM and clays (principally), as suggested by the presence of Si, Al, Mg, Ca and Na in the particles (Fig. 6b). Thus, the protection by the ‘mineral matrix’ is an operative mode of preservation at both sites but shows two different features depending on the core:

• In the shallow water core, mineral–OM association microfabrics occur as large clay or carbonate aggregates (pellets) of a few μm in diameter and containing discrete OM blebs of 0.1 μm in size as observerd by Ransom et al. (1998b) in samples from the nepheloid layer offshore California. Those pellets are typically observed in sample 120 (Fig. 5E and F)
• In the deep water core, the organo-mineral association is formed by apparently undifferentiated microaggregates (Fig. 5G–J). High magnification (×80,000) highlights, however, the ultrastructure of the micro-aggregates and reveals that OM is intimately associated with the surface of the clays as well as being in the interlayer spaces (Fig. 5I and K). The clay sheets appear completely embedded within the OM, contrasting with the monolayer clay–OM association traditionally described by Mayer (1994) or Collins et al. (1995), among others. Some pale flecks, tens of nm in size, are also seen in the highly magnified TEM images of deep core samples 1343 and 1513 (Fig. 5G). EDS pin-point analysis of these particles shows the elements of clays and carbonates, which is surprising considering the classic dark appearance of these minerals under an electron beam. We presently do not know if those particles contain any organic compounds or how they have resisted HF/HCl leaching.

OM aggregates were also observed by SEM in recent upwelling sediments from the northwest African slope. Their formation was ascribed to the degradation–recondensation process (Zegouagh et al., 1999). However, when viewed by TEM, this isolated OM appeared nanoscopically amorphous and resembled the NAOM shown on Fig. 5L. Aggregates from both the upper and the lower Namibian slope result from organo-mineral associations. NAOM formation, on the other hand, is ascribed to the sulfurization mechanism. However, considering the nanoscopically amorphous texture of melanoidin compounds (Zegouagh et al., 1999), we cannot dismiss the possibility that the degradation–recondensation mechanism also contributed to NAOM formation.

5.4. Oxygenation index (Iox) inferred from infrared spectroscopy

Infrared spectra show the distribution of major chemical bonds and their modes of vibration (Rouxhet et al., 1980). Subsequent to palynofacies description, 23 samples of isolated OM were analysed by FTIR. All exhibit essentially the same absorption bands, but the relative intensities differ, as shown in Fig. 7 and as described as follows:

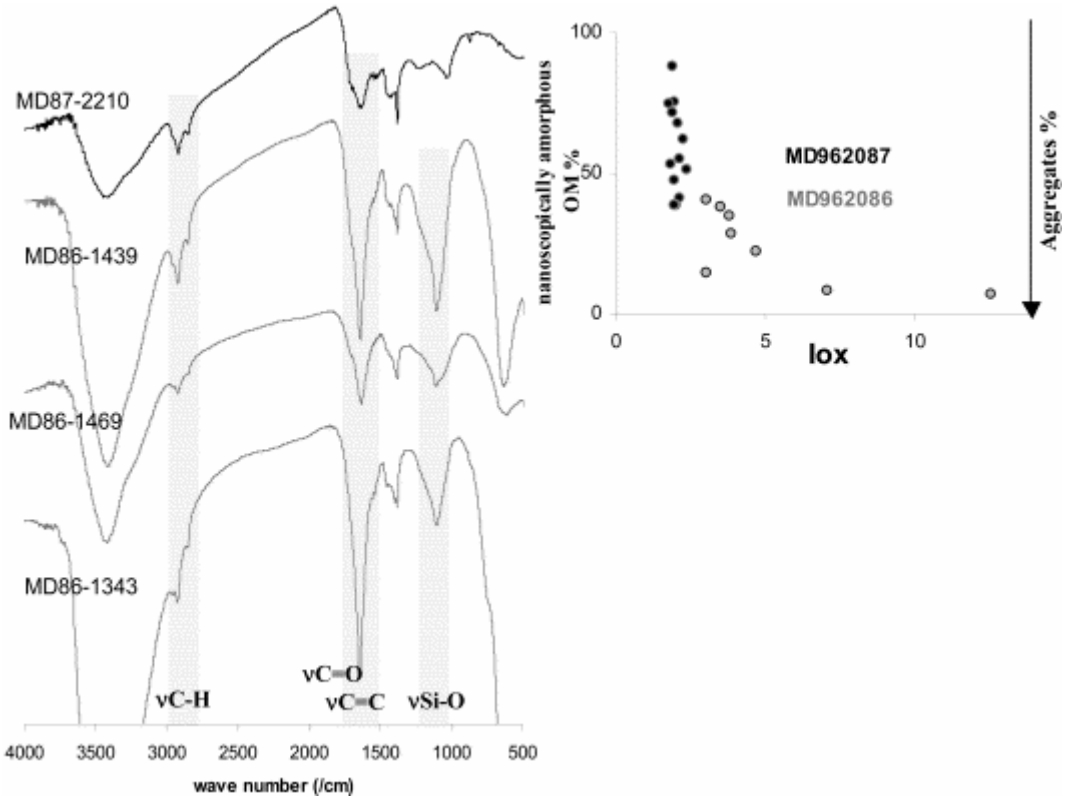

Fig. 7. FTIR spectra of isolated OM from MD962086 and MD962087. NAOM content of samples 2210, 1439, 1469 and 1343 are 51, 37.7, 28.5 and 8%, respectively, and TOC content before HF/HCl treatment were 6.7, 7.2, 2 and 1.6 wt.%. Iox are expressed *versus* NAOM contents, as% of palynofacies. One sample does not follow the trend and shows a lower NAOM contribution (14%) than expected considering the TOC content (2.95 wt.%) of the bulk sediment.

OM from the upper slope core (15 samples) has a broad band around 3430 cm^{-1}, characteristic of OH and molecular water stretching vibrations. Although the highly hydrophilic pellets were dried in a desiccator in order to avoid the effect of moisture, water was not efficiently removed from the KBr. As a result, the intensity of the band at 3430 cm^{-1} does not reflect the OH group abundance in OM. At 2930 and 2860 cm^{-1}, a well defined double band is due to the asymmetric and symmetric stretching of alkyl groups (CH_2, CH_3). Bending bands of CH_2 and CH_3 are seen around 1455 cm^{-1} and CH_3 bending at about 1380 cm^{-1}. Around 1710 cm^{-1}, a peak indicating the presence of C=O bonds from carbonyl and/or carboxyl functions appears as a shoulder on the 1630cm^{-1} band. This latter band is ascribed to C=C stretching of aromatics and alkene double bonds. All the IR spectra of the upper slope OM are similar irrespective of the TOC content and the relative amount of NAOM/aggregates in the samples.

Infrared spectra of the isolated OM from MD 962086 also show the above absorption bands but their relative intensity and shape differ from those of the shallow core spectra and vary according to TOC content and the petrographic composition of the samples. OM corresponding to organic-poor samples with low NAOM/aggregates ratios and slightly higher detrital OM contents yields weak alkyl bands and comparatively intense bands at 1630 cm^{-1}. Furthermore, an extra band around 1095 cm^{-1} is visible on all the spectra and corresponds to Si–O bonds typical of opal and clay crystals.

In order to constrain the differences between the IR absorptions and to assess the oxidation level of the OM, we calculated the Iox parameter (modified from Benalioulhaj and Trichet, 1990) as follows:

Clays and opal yield a band around 1600 cm^{-1}, which may result in an overestimation of the C=C, C=O stretching absorption intensity and hence affect Iox significance. However, this peak is one order of magnitude less intense than the peak around 1095 cm^{-1}. Thus, we assume that the overestimation of the C=C, C=O band at 1700–1630 cm^{-1} is low and does not invalidate Iox significance.

Spectra from the shallow core are relatively invariant; consequently, Iox is constant (Fig. 7, inset). This pattern is not surprising given the consistent petroleum quality observed in the core. In contrast, Iox of the lower slope OM is higher than for the upper slope and generally increases as the TOC content decreases. In the light of the Rock-Eval results, we suggest that the OM is more oxidized when accumulated on the lower slope than on the upper slope.

6. Implications

Two main preservation processes have acted on the Lüderitz slope with particular effectiveness and to a variable extent according to water depth and climate change.

6.1. Preservation processes: effects on OM quality

Organic matter from the shallow core appears mainly as NAOM, which is at least partly related to sulfurization. Adam et al. (2000) have reported the occurrence of sulfurization during early diagenesis off Walvis Bay. In addition, the 'degradation-recondensation' mechanism (Tissot and Welte, 1984) may have contributed to NAOM formation here. Organo-mineral associations and ultralaminae also exist on the upper slope, as shown by TEM observation, but they are minor constituents of the total OM. On the upper slope, the OM shows a consistently good petroleum quality (HI of 450 mg/g) and a low level of oxidation as evidenced by the low Iox and OI values. High contributions of sulfurized lipids on the upper slope can explain the good petroleum quality of the OM. Moreover, variations in the contribution of aggregates neither alter the petroleum quality nor enhance the oxidation level of the total OM. On the upper slope, both aggregation and sulfurization appear capable of preventing oxidation. Organic compounds deriving from degradation–recondensation processes have a low petroleum quality and presumably account for a minor fraction of the OM.

In the lower slope core, protection by aggregation is dominant. Sulfurization (and/or degradation–recondensation) does not play a major role, except for a few organic-rich levels from glacial isotopic stages 2–4 and 6, which have comparatively good petroleum quality and low extent of oxidation. Whether or not the good petroleum quality of these samples is related to the better efficiency of the sulfurization process compared to aggregation is debatable. Low sea level stands during glacial times may imply an offshore displacement of the upwelling cell and a faster export of OM to deep sites (Mollenhauer et al., 2002). Therefore, the duration of exposure to oxic

respiration for OM reaching a given depth was probably shorter during glacial periods than during high sea level stands. An alternative explanation would be related to the redox conditions at the sediment-water interface: enhanced melanoidin formation (by degradation–recondensation of saccharide and protein monomers) and decreased sulfurized lipid synthesis probably occurred during periods of low sulfate reduction, i.e. low OM flux to the sea floor. Variations in Iox and HI may be due to the predominance of melanoidin over organic sulfur compounds in NAOM rather than to an increased aggregates/NAOM ratio.

6.2. Relative contribution of different preservation processes: influence of organic and mineral fluxes

The percentage of organic carbon (OC) in the form of NAOM and aggregates (wt% bulk sediment) is shown on Fig. 8 and Fig. 9. The values were calculated by multiplying TOC content by the gel-like AOM contribution and the granular AOM (aggregates) contribution, respectively, determined using light microscopy. The percentage of OC protected by association with minerals is almost constant through time and between the two cores (0–4%), irrespective of TOC. NAOM contents vary, however, from almost 0 to >15% and are linearly correlated with TOC (Fig. 8). This suggests that factors controlling the occurrence of sulfurization reactions and the formation of aggregates are different.

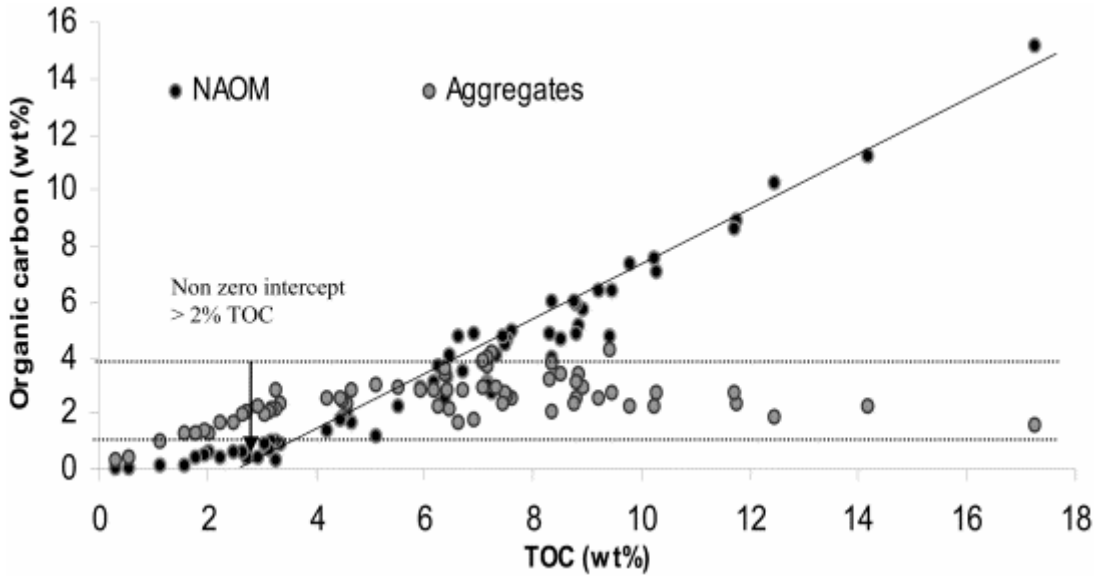

Fig. 8. Organic carbon (wt.% of bulk sediment) in the form of NAOM (black) and aggregates (grey) vs. TOC (wt.%); results from both cores are plotted together. NAOM is clearly correlated with TOC, while aggregates are invariant over the whole TOC range.

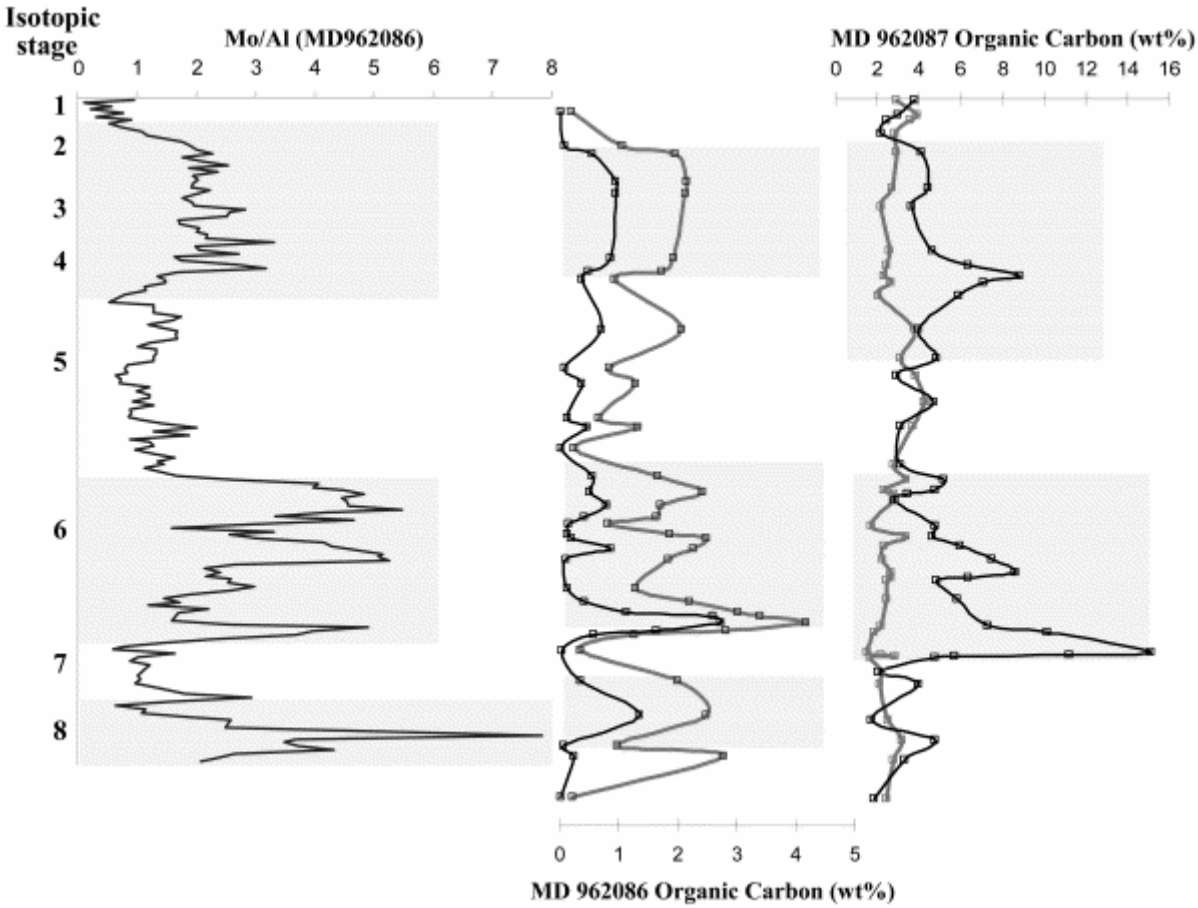

Fig. 9. Variation through time of TOC concentration (wt.% of bulk sediment) in the form of NAOM (black) and aggregates (grey) for MD 962087 and MD 962086. Also shown is the Mo/Al record of MD 962086, which can be interpreted as evidence of oxygen depletion in the surface sediments (Bertrand et al., 2002). Grey bands indicate glacial periods.

At both sites, the percentage of NAOM is greater during glacial periods (Fig. 9), when export fluxes to the slope were enhanced due to high primary productivity and/or low sea level stand (Mollenhauer et al., 2002). This could indicate that the effectiveness of NAOM formation depends, here, on the flux of labile OM reaching the sea floor. High OM fluxes drive intense oxygen utilization, accelerating the establishment of sulfidic conditions and hence the activation of sulfurization. The Mo:Al record (Bertrand et al., 2002, Fig. 9) of MD962086 suggests that the first centimetres of the sediment were depleted in oxygen during glacial periods and particularly during stage 6 (Crusius et al., 1996). This indicates that labile OM fluxes were enhanced at this time and sufficient to enable sulfurization even on the lower slope. Considering that upwelling perennially occurred over the shelf and upper slope (Lutjeharms and Meeuwis, 1987 and Dingle et al., 1996), we suggest that the redox conditions in the sediment were always favourable for sulfurization in the shallow-water core (Lückge et al., 1996). As a result, sulfurized lipids always dominate the NAOM in the upper slope. In addition, we consider that the degradation–recondensation process was also involved in NAOM formation, as previously emphasized. During periods of high fluxes of labile OM to the lower slope, the proportion of sulfurized lipids in the NAOM increased in response to enhanced bacterial sulphate reduction. As a corollary, melanoidin contribution to NAOM formation probably increased during periods of

moderate OM flux to the lower slope. This could explain the high Iox recorded during interglacial periods. Moreover, a substantial export flux is required to enable accumulation of organic matter as NAOM rather than aggregates, as suggested by the non-zero intercept (TOC>2%) shown in Fig. 8.

Aggregates occur in almost the same proportion at both water depths (between 0 and 4%). The abundance in the shallow-water core is quite constant over time and is clearly independent of climate-related changes in OM flux, in contrast to NAOM formation, which does apparently vary with OM flux. Like many authors (Mayer et al., 1988; Keil et al., 1994a; Keil et al., 1994b; Ransom et al., 1997 and Ransom et al., 1998a), we propose that the proportion of OC associated with the mineral fraction depends on the abundance of siliciclastic minerals (such as clays) and diatom frustules at the sediment-water interface and in the water column during deposition. Calculated percentages of OC involved in aggregates are correlated with biosilica+clay contents (Fig. 10) in the lower slope core; no correlation was found for the shallow core. The potential effect of carbonates in aggregation cannot be accurately estimated because of the intense diagenetic dissolution of this fraction. In addition, the collision frequency between particles and their stickiness related to the abundance of transparent exopolymer particles in sea water (Passow, 2002) may play an important role that is difficult to assess using sediment records.

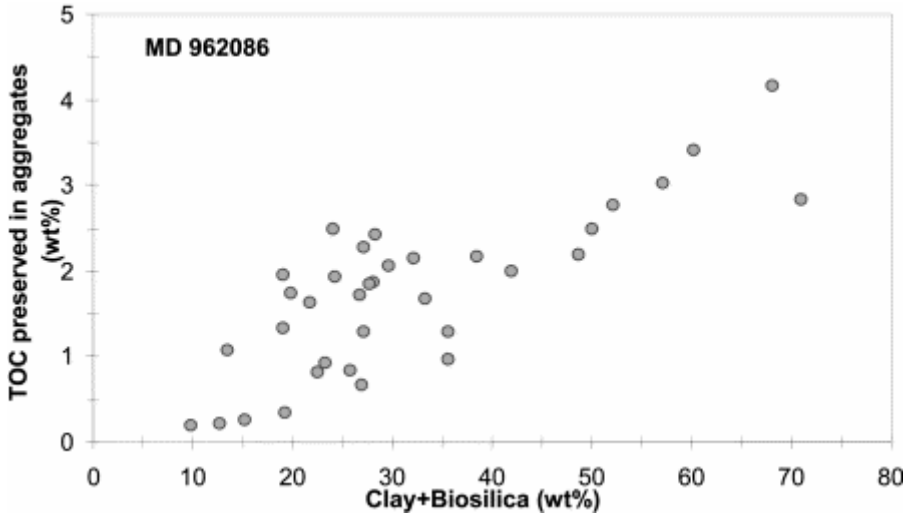

Fig. 10. TOC (wt.% of the bulk sediment) preserved by aggregation with minerals is weakly correlated with the Clay+Biosilica contents (wt.%) for the deep core. No correlation was found for the shallow core.

6.3. Limitation of aggregation

In the study area, protection by minerals seems to be unable to protect more TOC than 4% of the bulk sediment, even when OM fluxes were high (Fig. 8). During stage 6.6, for example, OM is mainly preserved through sulfurization (and/or degradation-recondensation), whereas organo-mineral associations only account for a few percent of the TOC. In the literature, only rare examples show cases of OM–mineral associations which permit TOC accumulation higher than 5% (see Salmon et al., 2000 and Keil et al., 1994b for exceptions). This suggests that, in the absence of other preservation pathways, the potential for aggregation (itself limited by mineral particle abundance and collision) to enhance OM accumulation is limited under high

rates of organic matter supply. Although recent studies show that thickening of OM particles tied to clay plates can enhance the preservation potential of minerals without increasing the surface occupied by OM (Bock and Mayer, 2000 and Arnarson and Keil, 2001), our results suggest a plateau in the effect of aggregation on OM accumulation, in the case of high OM supply.

On the lower slope, the formation of aggregates is limited, first by OM supply in case of low organic fluxes (OC in form of aggregates increases with TOC increasing from 0 to 4 wt.%, Fig. 8) and second, by mineral availability when organic matter delivery exceeds the loading ability of minerals. At the upper slope, contrary to the lower one, organic fluxes are never limiting. This would explain the apparent climate-driven variation in aggregate content in the deep sediments and the absence of such changes in the shallow sediments (Fig. 9).

6.4. Aggregate formation

Aggregates begin to form during sinking in the water column, as discussed by Alldredge and Silver (1988). Traditionally, aggregation is defined as the process by which faecal matter, microorganisms and mineral particles clump together to form larger particles that settle rapidly (McCave, 1984 and Alldredge and Silver, 1888). Hence, OM protection in mineral matrices probably begins in the surface layer. As a result, the percentage of OM preserved in the form of aggregates is almost equivalent at 1029 and 3606 m, and is independent of water depth and sinking time. Furthermore, in the case of low organic flux on the lower slope (during the Holocene and Eemian) only mineral–OM aggregates are seen in the sediments, while non-aggregated OM is almost completely absent. Non-ballasted OM has probably undergone drastic degradation in the water column due to the greater vulnerability and/or the slower sinking velocity of these particles. We propose that the aggregates observed on both the upper and lower slope originate from the pellets and marine snow that form in the water column, although disaggregation and re-aggregation phenomena in the benthic boundary layer probably occurred before burial and modified the structure of the aggregates (Ransom et al., 1998b). Marine snow is known to be fragile and prone to break-up in the benthic boundary layer (Thomsen and McCave, 2000). However, in case of low shear velocity (<1.6 cm s^{-1}) close to the sea floor, re-aggregation is promoted (Thomsen and McCave, 2000). Moreover, high sedimentation rates, such as those observed on the Namibian slope, enhance the burial efficiency of aggregates (Thomsen et al., 2002).

The size of water column aggregates depends on their ‘age’ (settling time) and on the concentration and types of discrete particles sinking in the surface, pelagic and nepheloid layers (Alldredge, 1998). According to Ransom et al. (1998b), a thick nepheloid layer facilitates aggregation, disaggregation and re-aggregation phenomena. Morphological differences between the upper and lower slope aggregates are clear: lower slope aggregates are smaller and denser (Fig. 5H) than those from the upper slope (Fig. 5E and F). This could be explained by the small size and sparseness of marine snow at the deep location and/or by the reduction of nepheloid layer thickness at greater depth (Giraudeau, personal communication). Both factors result from reduced productivity and OM flux off shore compared to near shore.

Also, the clay–OM association observed at 3606 m water depth and shown on the TEM micrographs, does not appear as patches or coating of organic compounds on clay particles: the clay crystals seem embedded in the amorphous OM. A so far undescribed pattern of aggregation between clay and OM may be displayed here, but further investigations are needed.

7. Conclusions

The application of different and complementary methods to a large number of samples and over extensive ranges of depth and time gives detailed information on the OM accumulated off Lüderitz and some insight into the factors and processes that mediate its preservation:

1. Biological structures, as cell walls and ultralaminae, related to the selective preservation mode, are observed at both sites but constitute a minor form of preserved OM on the slope.
2. Protection by aggregation with minerals occurs on both the lower and upper slopes but shows different features depending on depth. We suggest that this OM acquires resistance to degradation as aggregates formed during sinking. Aggregation appears to be an efficient preservation mode on the lower slope.
3. NAOM formation results from sulfurization and, presumably, degradation–recondensation reactions. NAOM accumulation depends on OM flux which controls the establishment of favourable suboxic conditions at the interface. This type of preserved OM dominates on the upper slope.

Lüderitz slope sediments are particularly rich in OM thanks to high surface productivity resulting from perennial upwelling, but also due to the occurrence of different OM preservation mechanisms operating in the sediment, at the sediment interface and presumably, during sinking. Two dominant preservation modes are recognized. Each yields particular forms of preserved OM which show a characteristic distribution on the slope. It is striking that preservation by organo-mineral association, although consistently operative through time at both depths, accounts for a relatively minor part of the OM accumulated on this organic-rich slope. It thus appears that, in the case of high organic fluxes, protection by aggregation has a limited effect on OM accumulation. Supplementary preservation mechanisms are required to permit TOC contents higher than ~4% in the sediment at this location.

Acknowledgements

This study was carried out within the framework of a collaboration between the Institut Français du Petrole (IFP), the Museum National d'Histoire Naturelle de Paris, the Département de Géologie et Océanographie de Bordeaux and the Laboratoire de Géologie de la Matière Organique d'Orléans. Total Fina Elf provided the financial support. The cores were retrieved during NAUSICAA cruise (IMAGE II) with the R/V Marion Dufresne, which was made available by IPEV. The authors are grateful to D. Keravis for technical assistance in performing Rock-Eval analyses and to F. Frölich for help in interpretations of FTIR spectra. We also thank E. Galbraith for editing and improving the english version and Drs. S. Wakeham and Y. Furukawa for constructive comments.

References

Adam, P., Schneckenburger, P., Schaeffer, P. and Albrecht, P., 2000. Clues to early diagenetic sulfurization processes from mild chemical cleavage of labile sulfur-rich geomacromolecules. *Geochimica et Cosmochimica Acta* **64**, pp. 3503–3585.

Alldredge, A.L. and Silver, M.W., 1888. Characteristic, dynamics and significance of marine snow. *Progress in Oceanography* **20**, pp. 41–82.

Alldredge, A., 1998. The carbon, nitrogen and mass content of marine snow as a function of aggregate size. *Deep-Sea Research I* **45**, pp. 529–541.

Armstrong, R.A., Lee, C., Hedges, J.I., Honjo, S. and Wakeham, S.G., 2002. A new, mechanistic model for organic carbon fluxes in the ocean based on quantitative association of POC with ballast minerals. *Deep-Sea Research II* **49**, pp. 219–236.

Arnarson, T.S. and Keil, R.G., 2001. Organic-mineral interactions in marine sediments studied using density fractionation and X-ray photoelectron spectroscopy. *Organic Geochemistry* **32**, pp. 1401–1415.

Barange, M. and Pillar, S.C., 1992. Cross-Shelf circulation, zonation and maintenance mechanisms of nyctiphanes-capensis and euphausia-hanseni (euphausiacea) in the Northern Benguela upwelling system. *Continental Shelf Research* **12**, pp. 1027–1042.

Behrenfeld, M.J. and Falkowski, P.G., 1997. Photosynthetic rates derived from satellite-based chlorophyll concentration. *Limnology and Oceanography* **42**, pp. 1–20.

Benalioulhaj, S. and Trichet, J., 1990. Comparative study by infra red spectroscopy of the organique matter of phosphate-rich (Oulad Abdoun basin) and black shale (Timadhit basin) series (Morocco). *Organic Geochemistry* **16**, pp. 649–660.

Bertrand, P., Giraudeau, J., Malaizé, B., Martinez, P., Gallinari, M., Pedersen, T.F., Pierre, C. and Venec-Peyré, M.-T., 2002. Occurrence of an exceptional carbonate dissolution episode during early glacial isotope stage 6 in the Southern Atlantic. *Marine Geology* **180**, pp. 235–248.

Bertrand, P., Pedersen, T.F., Schneider, R., Shimmield, G., Lallier-Verges, E., Disnar, J.-R., Massias, D., Villanueva, J., Tribovillard, N., Huc, A.Y., Giraud, X., Pierre, C. and Venec-Peyre, M.-T., 2003. Organic-rich sediments in ventilated deep-sea environments: relationship to climate, sea level, and trophic changes. *Journal of Geophysical Research* **108**, pp. 1–11.

Bock, M.J. and Mayer, L.M., 2000. Mesodensity organo-clay associations in a near-shore sediment. *Marine Geology* **163**, pp. 65–75.

Boussafir, M., Lallier-Vergès, E., Bertrand, P. and Badaut-Trauth, D., 1994. Structure ultrafine de la matière organique des roches mères du Kimmeridgien du Yorkshire (UK). *Bulletin of the Geological Society France* **165**, pp. 355–363.

Boussafir, M., Gelin, F., Lallier-Vergès, E., Derenne, S., Bertrand, P. and Largeau, C., 1995. Electron microscopy and pyrolysis of kerogens from the Kimmeridge Clay Formation, UK: source organisms, preservation processes, and origin of microcycles. *Geochimica et Cosmochimica Acta* **59**, pp. 3731–3747.

Boussafir, M. and Lallier-Vergès, E., 1996. Accumulation of organic matter in the Kimmeridge Clay Formation (KCF): an update fossilisation model for marine petroleum source-rocks. *Marine and Petroleum Geology* **14**, pp. 75–83.

Calvert, S.E. and Pedersen, T.F., 1993. Geochemistry of Recent oxic and anoxic marine sediments: Implications for the geological record. *Marine Geology113*, pp. 67–88.

Canfield, D.E., 1993. Organic matter oxidation in marine sediments. In: Wollast, R., Mackenzie, F.T. and Chou, L., Editors, 1993. *Interactions of C, N, P and S Biogeochemical Cycles and Global Changes. NATO Series*, Springer, Berlin, pp. 1–61.

Collins, M.J., Bishop, A.N. and Farrimond, P., 1995. Sorption by mineral surfaces: rebirth of the classical condensation pathway for kerogen formation?. *Geochimica et Cosmochimica Acta* **59**, pp. 2387–2391.

Crusius, J., Calvert, S., Pedersen, T. and Sage, D., 1996. Rhenium and molybdenum enrichments in sediments as indicators of oxic, suboxic and sulfidic conditions of deposition. *Earth and Planetary Science Letters* **145**, pp. 65–78.

Derenne, S., Le Berre, F., Largeau, C., Hatcher, P., Connan, J. and Raynaud, J.F., 1991. Formation of ultralaminae in marine kerogens via selective preservation of thin resistant outer walls of microalgae. *Organic Geochemistry* **19**, pp. 345–350.

Derenne, S., Largeau, C., Hetényi, M., Brukner-Wein, A., Connan, J. and Lugardon, B., 1997. Chemical structure of the organic matter in a Pliocene maar-type shale: Implicated Botryococcus race strains and formation pathways. *Geochimica et Cosmochimica Acta* **61**, pp. 1879–1889.

Dingle, R.V., Bremner, J.M., Giraudeau, J. and Buhmann, D., 1996. Modern and palaeo-oceanographic environments under Benguela upwelling cells off southern Namibia. *Palaeogeography Palaeoclimatology Palaeoecology* **123**, pp. 85–105.

Durand, B. and Nicaise, G., 1980. Procedures for kerogen isolation. In: Durand, B., Editor, , 1980. *Kerogen*, Technip, Paris, pp. 33–53.

Espitalié, J., Deroo, G. and Marquis, F., 1985. La pyrolyse Rock-Eval et ses applications; première partie. *Revue de l'Institut Français du Pétrole* **40**, pp. 563–579.

Furukawa, Y., 2000. Energy-filtering transmition electron microscopy (EFTEM) and electron energy loss spectroscopy (EELS) investigation of clay-organic matter aggregates in aquatic sediments. *Organic Geochemistry* **31**, pp. 735–744.

Giraudeau, J. and Bailey, G.W., 1995. Spatial dynamics of coccolithophore communities during an upwelling event in the Southern Benguela system. *Continental Shelf Research* **15**, pp. 1825–1852.

Hagen, E., Feistel, R., Agenbag, J.J. and Ohde, T., 2001. Seasonal and interannual changes in Intense Benguela Upwelling (1982–1999). *Oceanologica Acta* **24**, pp. 557–568.

Hedges, J.I. and Keil, R.G., 1999. Organic geochemical perspectives on estuarine processes: sorption reactions and consequences. *Marine Chemistry* **65**, pp. 55–65.

Hedges, J.I., Baldock, J.A., Gelinas, Y., Lee, C., Peterson, M. and Wakeham, S.G., 2001. Evidence for non-selective preservation of organic matter in sinking marine particles. *Nature* **409**, pp. 801–804.

Hedges, J.I., Hu, F.S., Devol, A.H., Hartnett, H.E., Tsamakis, E. and Keil, R.G., 1999. Sedimentary organic matter preservation: a test for selective degradation under oxic conditions. *American Journal of Science* **299**, pp. 529–555.

Imbrie, J., Hays, J.D., Martinson, D.G., McIntyre, A., Mix, A.C., Morley, J.J., Pisias, N.G., Prell, W.L. and Shackleton, N.J., 1984. The orbital theory of Pleistocene climate support from a revised chronology of the marine δ18O record. In: Berger, A.L., Imbrie, J., Hays, J., Kukla, G. and Saltzman, B., Editors, 1984. *Milankovitz and Climate*, D. Reidel, Norwell, MA, pp. 269–305.

Keil, R.G., Montluçon, D.B., Prahl, F.G. and Hedges, J.I., 1994. Sorptive preservation of labile organic matter in marine sediments. *Nature* **370**, pp. 549–552.

Keil, R.G., Tsamakis, E., Fuh, C.B., Giddings, J.C. and Hedges, J.I., 1994. Mineralogical and textural controls on the organic composition of coastal marine sediments: hydrodynamic separation using SPLITT-fractionation. *Geochimica et Cosmochimica Acta* **58**, pp. 879–893.

Kirst, G.J., Schneider, R.R., Müller, P.J., von Storch, I. and Wefer, G., 1999. Late quaternary temperature variability in the Benguela current system derived from alkenones. *Quaternary Research* **52**, pp. 92–103.

Kok, M.D., Schouten, S. and Sinninghe-Damsté, J.S., 2000. Formation of insoluble, non hydrolyzable, sulfur-rich macromolecules via incorporation of inorganic sulfur species into algal carbohydrates. *Geochimica et Cosmochimica Acta* **64**, pp. 2689–2699.

Largeau, C., Casadevall, E., Kadouri, A. and Metzger, P., 1984. Formation of Botryococcus Braunii kerogens. Comparative study of immature torbanite and the extant alga Botryococcus Braunii. In: Schenk, P.A., de Leeuw, J.W. and Lijmbach, G.W.M., Editors, 1984. *Advances in Organic Geochemistry 1983 Organic Geochemistry 8*, Pergamon Press, Oxford, pp. 327–332.

Largeau, C., Derenne, S., Casadevall, E. and Kadouri, A., 1986. Pyrolysis of immature Torbanite and of the resistant biopolymer (PRB A) isolated from extant alga

Botryococcus Braunii. Mechanism of formation and structure of Torbanite. In: Leythaeuser, D. and Rullkötter, J., Editors, 1986. *Advances in Organic Geochemistry 1985, Organic Geochemistry 10*, Pergamon Press, Oxford, pp. 1023–1032.

Largeau, C., Derenne, S., Casadevall, E., Berkaloff, C., Corolleur, M., Lugardon, B., Raynaud, J.F. and Connan, J., 1989. Occurence and origin of 'ultralaminar' structures in 'amorphous' kerogens of various source rocks and oil shales. *Organic Geochemistry* **16**, pp. 889–895.

Lückge, A., Horsfield, B., Littke, R. and Scheeder, G., 2002. Organic matter preservation and sulfur uptake in sediments from the continental margin of Pakistan. *Organic Geochemistry* **33**, pp. 477–488.

Lückge, A., Boussafir, M., Lallier-Vergès, E. and Littke, R., 1996. Comparative study of organic matter presevation in immature sediments along the continental margins of Peru and Oman. Part I: Results of petrographical and bulk geochemical data. *Organic Geochemistry* **24**, pp. 437–451.

Lutjeharms, J.R.E. and Meeuwis, J.M., 1987. The extent and variability of South-East Atlantic upwelling. *South African Journal of Marine Science* **5**, pp. 51–62.

Mayer, L.M., Rahaim, P.T., Guerin, W., Macko, S.A., Waltling, L. and Adersen, F.E., 1985. Biological and granulometric controls on sedimentary organic matter of an intertidal mudflat. *Estuarine and Coastal Shelf Science* **20**, pp. 491–504.

Mayer, L.M., Macko, S.A. and Cammen, L., 1988. Provenance, concentration and nature of sedimentary organic nitrogen in the Gulf of Maine. *Marine Chemistry* **25**, pp. 291–304.

Mayer, L.M., 1993. Organic matter at the sediment-water interface. In: Engel, M.H. and Macko, S.A., Editors, 1993. *Organic Geochemistry Principles and Applications*, Plenum Press, London, pp. 171–184.

Mayer, L.M., 1994. Surface area control of organic carbon accumulation in continental shelf sediments. *Geochimica et Cosmochimica Acta* **58**, pp. 1271–1284.

Mayer, L.M., 1999. Extent of coverage of mineral surfaces by organic matter in marine sediments. *Geochimica et Cosmochimica Acta* **63**, pp. 207–215.

McCave, I.N., 1984. Size spectra and aggregation of suspended particles in the deep ocean. *Deep-Sea Research I* **31**, pp. 329–352.

Mollenhauer, G., Schneider, R.R., Muller, P.J., Spiess, V. and Wefer, G., 2002. Glacial/interglacial variablity in the Benguela upwelling system: Spatial distribution and budgets of organic carbon accumulation. *Global Biogeochemical Cycles* **16**, pp. 1–5.

Mongenot, T., Derenne, S., Largeau, C., Tribovillard, N.P., Lallier-Vergès, E., Dessort, D. and Connan, J., 1999. Spectroscopic, kinetic and pyrolytic studies of

kerogen from the dark parallel laminae facies of the sulfur-rich Orbagnoux deposit (Upper Kimmeridgian, Jura). *Organic Geochemistry* **30**, pp. 39–56.

Oades, J.M., 1988. The retention of organic matter in soil. *Bio-Geochemistry* **5**, pp. 35–70.

Passow, U., 2002. Transparent exopolymer particles (TEP) in aquatic environments. *Progress in Oceanography* **55**, pp. 287–333.

Ramanampisoa, L. and Disnar, J.R., 1994. Primary control of paleoproduction on organic matter preservation and accumulation in the Kimmeridge rocks of Yorshire (UK). *Organic Geochemistry* **21**, pp. 1153–1167.

Ransom, B., Bennett, R.H., Bearwald, R. and Shea, K., 1997. TEM study of in situ organic matter on continental margins: occurence and the 'monolayer' hypothesis. *Marine Geology* **138**, pp. 1–9.

Ransom, B., Dongseon, K., Kastner, M. and Wainwright, S., 1998. Organic matter preservation on continental slopes: importance of mineralogy and surface area. *Geochimica et Cosmochimica Acta* **62**, pp. 1329–1345.

Ransom, B., Shea, K.F., Burkett, P.J., Bennett, R.H. and Baerwald, R., 1998. Comparison of pelagic and nepheloid layer marine snow: implications for carbon cycling. *Marine Geology* **150**, pp. 39–50.

Rouxhet, P.G., Robin, P.L. and Nicaise, G., 1980. Characterisation of kerogens and their evolution by infrared spectroscopy. In: Durand, I.F.P., Editor, , 1980. *Insoluble Organic Matter from Sedimentary Rocks*, TECHNIP, Paris, pp. 163–190.

Saint-Germes, M., Baudin, F., Bazhenova, O., Derenne, S., Fadeeva, N. and Largeau, C., 2002. Origin and preservation processes of amorphous organic matter in the Maykop Series (Oligocene-Lower Miocene) of Precaucasus and Azerbaijan. *Bulletin de La Societé Géologique de France* **175**, pp. 423–436.

Salmon, V., Derenne, S., Lallier-Vergès, E., Largeau, C. and Beaudoin, B., 2000. Protection of organic matter by mineral matrix in a Cenomanian black shale. *Organic Geochemistry* **31**, pp. 463–474.

Schouten, S., vanDriel, G.B., Sinnighe Damsté, J.S. and de Leeuw, J.W., 1994. Natural sulfurisation of ketones and aldehydes: A key reaction in the formation of organic sulfur compounds. *Geochimica et Cosmochimica Acta* **57**, pp. 5111–5116.

Schulz, H.D., Dahmke, A., Schinzel, U., Wallmann, K. and Zabel, M., 1994. Early diagenetic processes, fluxes, and reaction rates in sediments of the South Atlantic. *Geochimica et Cosmochimica Acta* **58**, pp. 2041–2060.

Shannon, L.V. and Nelson, G., 1996. The Benguela: large scale features and processes and system variability. In: Wefer, G., Berger, W.H., Siedler, G. and Webb, D., Editors, 1996. *The South Atlantic Ocean, Present and Past Circulation*, Springer, Berlin, pp. 163–210.

Sinninghe-Damsté, J.S., Ripjstra, W.I.C., Kock-van Dalen, A.C., de Leeuw, J.W. and Schenck, P.A., 1989. Quenching of labile functionalized lipids by inorganic sulfur species: Evidence for formation of sedimentary organic sulfur compounds at the early stage of diagenesis. *Geochimica et Cosmochimica Acta* **53**, pp. 1343–1355.

Stuiver, M., Reimer, P.J., Bard, E., Beck, J.W., Burr, G.S., Hughen, K.A., Kromer, B., McCormick, G., van der Plicht, J. and Spurk, M., 1998. INTCAL98 radiocarbon age calibration, 24,000-0 cal BP. *Radiocarbon* **40**, pp. 1041–1083.

Suess, E., 1973. Interaction of organic compounds with calcium carbonates, II. Organo-carbonate associations in recent sediments. *Geochimica et Cosmochimica Acta* **37**, pp. 2435–2447.

Tegelaar, E.W., de Leeuw, J.W., Derenne, S. and Largeau, C., 1989. Reappraisal of kerogen formation. *Geochimica et Cosmochimica Acta* **53**, pp. 3103–3106.

Thomsen, L., vanWeering, T. and Gust, G., 2002. Processes in the benthic boundary layer at the Iberian continental margin and their implication for carbon mineralization. *Progress in Oceanography* **52**, pp. 315–329.

Thomsen, L.A. and McCave, I.N., 2000. Aggregation processes in the benthic boundary layer at the Celtic Sea continental margin. *Deep-Sea Research Part I-Oceanographic Research Papers* **47**, pp. 1389–1404.

Tissot, B.P. and Welte, D.H., 1984. Petroleum, Formation and Occurrence. , Springer, Berlin.

Wakeham, S., Sinninghe-Damsté, J.S., Kohnen, M.E.L. and de Leeuw, J.W., 1995. Organic sulfur compounds formed during early diagenesis in the Black Sea. *Geochimica et Cosmochimica Acta* **59**, pp. 521–533.

Wakeham, S.G., Lee, C., Hedges, J.I., Hernes, P.J. and Peterson, M.L., 1997. Molecular indicators of diagenetic status in marine organic matter. *Geochimica et Cosmochimica Acta* **61**, pp. 5363–5369.

Zegouagh, Y., Derenne, S., Largeau, C., Bertrand, P., Sicre, M.A., Saliot, A. and Rousseau, B., 1999. Refractory organic matter in sediments from the North-West African upwelling system: abundance, chemical structure and origin. *Organic Geochemistry* **30**, pp. 101–117.